KCNE1 is an auxiliary subunit of two distinct ion channel superfamilies

Pablo Ávalos Prado, Stephanie Häfner, Yannick Comoglio, Brigitte Wdziekonski, Christophe Duranton, Bernard Attali, Jacques Barhanin, Guillaume Sandoz

KCNE1 is an auxiliary subunit of two distinct ion channel superfamilies

Authors: Pablo Ávalos Prado[1,2], Stephanie Häfner[1,2], Yannick Comoglio[1,2], Brigitte Wdziekonski[1,2], Christophe Duranton[2,3], Bernard Attali[4], Jacques Barhanin[2,3] and Guillaume Sandoz*[1,2,5]

Affiliations:

[1]Université Cote d'Azur, CNRS, INSERM, iBV, France

[2]Laboratories of Excellence, Ion Channel Science and Therapeutics Nice, France

[3]Université Côte d'Azur, CNRS, LP2M, Medical Faculty, France

[4]Department of Physiology & Pharmacology, Sackler Faculty of Medicine and Sagol School of Neurosciences, Tel Aviv University, Tel Aviv, Israel.

[5]Lead contact

*Correspondence to: sandoz@unice.fr

SUMMARY

Determination of what is the specificity of subunits composing a protein complex is essential when studying gene variants on human pathophysiology. The pore-forming α-subunit KCNQ1, which belongs to the voltage-gated ion channel superfamily, associates to its β-auxiliary subunit KCNE1 to generate the slow cardiac potassium I_{Ks} current, whose dysfunction leads to cardiac arrhythmia. Using pharmacology, gene invalidation and single molecule fluorescence assays, we found that KCNE1 fulfils all criteria of a *bona fide* auxiliary subunit of the TMEM16A chloride channel, which belongs to the anoctamin superfamily. Strikingly, assembly with KCNE1 switches TMEM16A from a calcium-dependent to a voltage-dependent ion channel. Importantly, clinically relevant inherited mutations within the TMEM16A-regulating domain of KCNE1 abolish the TMEM16A modulation, suggesting that the TMEM16A-KCNE1 current may contribute to inherited pathologies. Altogether, these findings challenge the dogma of the specificity of auxiliary subunits regarding protein complexes and questions ion channel classification.

KEYWORDS

Ancillary subunits, Anoctamin, KCNE1, Potassium channel, MinK1, IsK, Proximal convoluted tubule cells, Voltage-dependent ion channels, Protein complexes, Single molecule fluorescence.

INTRODUCTION

KCNE1 is a 129-residue peptide, with a single short hydrophobic membrane spanning domain and carboxy- and amino-terminal domains facing towards the intracellular and extracellular side, respectively (Takumi et al., 1988). When injected in *Xenopus laevis* oocytes, KCNE1 produces a slowly activating K^+ current (Takumi et al., 1988). For this reason, KCNE1 was initially believed to be the minimal sequence that could encode for a K^+ channel (Goldstein and Miller, 1991; Wang and Goldstein, 1995). Experiments using other heterologous cell models questioned this finding since expression of KCNE1 alone is not able to induce current in mammalian cell lines (Lesage et al., 1993). This enigma was resolved by the discovery that *Xenopus* oocytes express endogenous KCNQ1 channels, which are modulated by KCNE1 (Barhanin et al., 1996; Sanguinetti et al., 1996). These experiments showed that KCNE1 does not encode for a pore-forming α -subunit but for an ancillary (β) subunit of the voltage-dependent potassium KCNQ1 channel. Association between KCNQ1 and KCNE1 underlies the slow repolarizing component in the cardiac action potential (I_{Ks}) (Barhanin et al., 1996; Sanguinetti et al., 1996). In addition to the K^+ current described above, a voltage-dependent Cl^- current was observed upon injection of cRNA of KCNE1 in *Xenopus* oocytes (Attali et al., 1993), and up to now, the molecular identity of this current has remained elusive.

Ca^{2+}-activated Cl^- channels (CaCCs), belonging to the anoctamin protein superfamily, play a major role in cell physiology, including signal transduction, regulation of cardiac and neuronal excitability, epithelial secretion and muscle contraction, among others (Hartzell et al., 2005; Pedemonte and Galietta, 2014). TMEM16A was the first member of this superfamily to be cloned by three independent laboratories, using different approaches (Caputo et al., 2008; Schroeder et al., 2008; Yang et al., 2008). Ten anoctamin members have been found in mammals, but only TMEM16A and TMEM16B have been demonstrated to be full CaCCs, whereas the rest of the family operate as scramblases that rapidly and bidirectionally translocate lipids maintaining the asymmetry of the plasma membrane (Falzone et al., 2018; Pedemonte and Galietta, 2014). The structure of TMEM16A has been recently elucidated, defining the channel as a homodimer constituted of ten transmembrane domains per subunit (Dang et al., 2017; Peters et al., 2018). TMEM16A represents the major chloride channel in *Xenopus* oocytes (Schroeder et al., 2008), where it mediates fast polyspermy block (Wozniak et al., 2018). Nevertheless, no β-subunit has been identified for this channel up to now.

Because of its high expression in *Xenopus* oocytes (Schroeder et al., 2008), we hypothesize in the present manuscript that KCNE1 may serve as a β-subunit of the pore-forming TMEM16A α-subunits to induce the voltage-gated Cl^- current, which was described almost 30 years ago (Attali et al., 1993). We demonstrate here that KCNE1 interacts physically with TMEM16A with a 2α:2β stoichiometry using electrophysiology in heterologous and native systems and single molecule pulldown assays. This interaction induces a sustained voltage-dependent chloride current in the absence of elevated cytoplasmic Ca^{2+}, which, physiologically, responds to the blood pressure regulating renin-angiotensin system in proximal tubule cells. Importantly, we find that clinically relevant inherited polymorphisms within the KCNE1-regulating domain, including the common S38G polymorphism, abolish the KCNE1-dependent regulation of TMEM16A, indicating that this current may contribute to inherited pathologies such as cardiac arrhythmia. Our results demonstrate that KCNE1 fulfils all criteria of an auxiliary subunit of chloride channels. This is the very first example of an auxiliary subunit that associates with and modulates two distinct classes of protein superfamilies: the voltage-gated ion channels and the anoctamins. This novel finding should be considered when analyzing functional impacts of KCNE1 gene variants on human pathophysiology.

RESULTS

KCNE1 shifts TMEM16A from a calcium dependent to a voltage-dependent Cl^- channel

To test the ability of KCNE1 to regulate TMEM16A, we used the heterologous HEK293T cell model, which expresses neither TMEM16A nor KCNE1 endogenously. Whereas transfection of HEK293T cells with either TMEM16A or KCNE1 alone produced no significant current, co-expression of both proteins induced a voltage-dependent current, whose density was of 18.1 ± 2.8 pA/pF at +100 mV (**Figures 1A and 1B**). The reversal potential was -4.8 ± 1.3 mV, which is similar to the expected reversal Cl^- potential in the experimental conditions used. This chloride current was inhibited by niflumic acid (NFA), T16Ainh-A01 (Davis et al., 2013) and also by Ani9, the most specific TMEM16A inhibitor (Seo et al., 2016) (**Figures 1C and 1D**). As expected, the TMEM16A-KCNE1 current presented higher permeability for large anions with lower hydration energy, as it has been shown before for TMEM16A alone in the presence of calcium (**Table 1**) (Caputo et al., 2008; Schroeder et al., 2008; Yang et al., 2008). In addition, the channel does not become cation permeable, since replacement of the external solution by a 15 mM NaCl solution supplemented with D-mannitol

allowed us to determine a P_{Na}/P_{Cl} of ~0.1. This value is consistent with the calculated prediction through the Goldman-Hodgkin-Katz equation in our conditions (see **Equation 1, STAR Methods**) and similar to the reported value (Yang et al., 2008; Peters et al., 2018). This suggests that KCNE1 switches TMEM16A from a calcium-dependent to a voltage-dependent chloride channel.

To preclude the possibility that KCNE1 activates endogenous calcium channels, we conducted similar experiments in the presence of the fast calcium chelator BAPTA (**Figures 1E and 1F**). As shown in **Figure 1F**, BAPTA did not affect the voltage-dependent current evoked by the TMEM16A-KCNE1 complex. To rule out a potential modulation of endogenous calcium channels by KCNE1 leading to TMEM16A activation, we co-expressed KCNE1 with the Ca^{2+}-activated SK4 channel, which has a similar calcium sensitivity as TMEM16A (Cao and Houamed, 1999). KCNE1 overexpression did not induce any increase of the SK4 current in the absence of calcium (**Figure S1**). Altogether, these results exclude an implication of intracellular Ca^{2+} in the KCNE1-induced and voltage-dependent activation of TMEM16A.

TMEM16A does not have any obvious classical voltage-sensor domains, but several cytoplasmic and transmembrane domains have been shown to be implicated in its regulation by voltage, including the first intracellular loop (Xiao et al., 2011) and the sixth transmembrane domain (TM6) (Peters et al., 2018). To determine, which domain is involved in the KCNE1-induced voltage-gating of the channel, we first tested the effect of KCNE1 on the mutation $_{444}$EEEE$_{447}$/$_{444}$AAAA$_{447}$ that is known to abolish the intrinsic TMEM16A voltage-dependence (Xiao et al., 2011). The mutation $_{444}$EEEE$_{447}$/$_{444}$AAAA$_{447}$ did not prevent channel regulation by KCNE1, ruling out the hypothesis that KCNE1 modifies the gating of TMEM16A by acting on the intrinsic voltage-dependence linked to this domain (**Figure S2**). We then tested the role of the TMEM16A TM6 domain using two TMEM16A mutants bearing the TM6 mutations I637A and Q645A, which enable the channel to be activated in the absence of calcium (Peters et al., 2018). As expected, these two mutants produced current in the absence of elevated Ca^{2+}, but no additional effect was observed upon co-expression of KCNE1 (**Figures 2A-C**). The absence of an additive effect strongly supports the idea that KCNE1 modulates channel gating by acting on the TM6 conformation. This conformation mimics a single Ca^{2+} occupancy state as has been demonstrated for both mutations (**Figures 2B and 2C**) (Peters et al., 2018). Supporting this, we found that the conductance versus Vm curve observed for TMEM16A + KCNE1 overlaps with the curve obtained with TMEM16A alone at moderate calcium concentrations (0.5 µM; **Figure 2D**). Despite of their ability to enable channel activation in the absence of calcium, the TM6

I637A and Q645A mutants are still modulated by Ca^{2+} (Peters et al., 2018). Therefore, we assessed the calcium sensitivity of the TMEM16A-KCNE1 current. Similarly to both mutants, TMEM16A-KCNE1 presented a calcium sensitivity (**Figure 2E and 2F and S3**) reinforcing the idea that KCNE1 modulates channel gating by acting on the TM6 conformation. We also evaluated the impact of KCNE1 co-expression on channel density and found that there was no effect of KCNE1 on it. In fact, at saturating calcium concentrations no difference in current densities was observed between cells expressing TMEM16A alone and TMEM16A + KCNE1 (**Figure 2F**).

TMEM16A activation by KCNE1 involves physical interaction

To be considered as an auxiliary subunit, a protein has to interact directly and stably with the α-subunits. To test the physical association between KCNE1 and TMEM16A, we used the recently developed single molecule pull-down (SiMPull) assay (Jain et al., 2011; Levitz et al., 2016; Royal et al., 2019). By direct visualization of antibody-immobilized protein complexes (**Figures 3A and 3E**), this technique allows one to determine the composition and stoichiometry within single protein complexes by counting fluorophore bleaching (Jain et al., 2011; Levitz et al., 2016; Royal et al., 2019). After co-transfection with the two putative partners KCNE1 and TMEM16A, one of them fused to an HA affinity tag and the other to a GFP label, and subsequent pull-down, we observed many fluorescent spots for both conditions, TMEM16A-GFP + HA-KCNE1 (**Figure 3B**) and KCNE1-GFP + HA-TMEM16A (**Figure 3F**). This demonstrates a physical interaction between KCNE1 and TMEM16A. Importantly, when HA-KCNE1 or HA-TMEM16A were not co-expressed, no proteins fused to GFP were isolated (**Figures 3I-L**), confirming the specificity of the HA-antibody that we used in our SiMPull assays. By analyzing bleaching steps for immobilized HA-KCNE1-TMEM16A-GFP complexes, we were able to determine the number of TMEM16A-GFP subunits within the complex. We found that the majority of fluorescence intensity trajectories showed two-step bleaching (~70%), with the remaining spots bleaching in one step (~20%) or occasionally three steps (~10%) (**Figures 3C and 3D**). This distribution agrees well with the binomial distribution predicted for a strict dimer based on an estimated GFP maturation probability of ~75% (Ulbrich and Isacoff, 2007). Analysis of the SiMPull experiment with HA-TMEM16A-KCNE1-GFP showed that most complexes presented two bleaching steps (~65%) and some remaining spots bleached in one (~25%) and three steps (~10 %) (**Figures 3G and 3H**). This distribution corresponds to the presence of two KCNE1-GFP subunits within the protein complex.

Therefore, two KCNE1 subunits assemble with two TMEM16A subunits (Dang et al., 2017; Takumi et al., 1988), following a 2α:2β stoichiometry.

The KCNEs-dependent regulation of TMEM16A is not restricted to KCNE1

The anoctamin family is constituted of ten members, but only TMEM16A and TMEM16B have been demonstrated to be full CaCCs (Schroeder et al., 2008). We assessed the ability of the KCNE1 to modulate the TMEM16B current. Co-expression of TMEM16B with KCNE1 did not induce any chloride current at rest, nor did any other KCNE subunit (**Figure S4A**). The KCNE family comprises five members which show a similar structure despite their low homology (Crump and Abbott, 2014). The different members of this family have been found to differently regulate the KCNQ1 channel (Bendahhou et al., 2005). We studied TMEM16A regulation by the different KCNE subunits and observed that, as demonstrated for KCNE1, only KCNE5 was able to induce a sustained chloride current in the absence of intracellular elevation of Ca^{2+} (**Figure S4B and S4C**). KCNE5 was also found to interact with TMEM16A at the single molecule level (**Figure S4D and S4E**).

The complex KCNE1-TMEM16A generates voltage-dependent Cl^- currents in proximal convoluted tubule cells

To be considered as a *bona fide* auxiliary subunit, the protein must interact with the alpha subunits in a native environment. To confirm that KCNE1 is an auxiliary subunit of TMEM16A in native tissue and to eliminate possible artifacts due to heterologous overexpression, we took advantage of kidney proximal convoluted tubule (PCT) cells obtained from wild type and *kcne1* KO mice (Barrière et al., 2003). PCT cells are considered as a relevant model as they naturally co-express both TMEM16A and KCNE1 (Faria et al., 2014; Vallon et al., 2001) and do not necessitate any genetic manipulation to record TMEM16A currents. Moreover, while no modification of the K^+ current was found in PCT cells from *kcne1* KO mice compared to wild type, a DIDS (4,4'-Diisothiocyanostilbene-2,2'-disulfonic acid)-sensitive Cl^- conductance was impaired (Barrière et al., 2003). We confirmed the loss of current, whose reversal potential was similar to the expected Cl^- reversal potential in *kcne1* null PCT cells (18.07 ± 1.21 pA/pF vs 5.37 ± 0.56 pA/pF for PCT wild type and KO mice, respectively) (**Figure 4A**). This current was inhibited by NFA (4.51 ± 0.28 pA/pF), T16Ainh-A01 (5.52 ± 0.72 pA/pF) and Ani9 (2.88 ± 0.38 pA/pF) (**Figures 4B-D**). Moreover, knock-down of

TMEM16A by a previously validated siRNA transfection (Sala-Rabanal et al., 2017) in wild type PCT cells significantly reduced the Cl^- current amplitude (4.23 ± 0.48 pA/pF) (**Figure 4E**). This demonstrates the involvement of TMEM16A subunits in the channel complex responsible for the herein studied Cl^- current. A rescue experiment by KCNE1 transfection of *kcne1*$^{-/-}$ cells fully restored the voltage-dependent Cl^- current (21.59 ± 1.38 pA/pF) (**Figure 4F**), showing that the absence of chloride current in these cells was only due to the KO of *kcne1* and not due to any modification that might occur during the culture process.

The KCNE1-TMEM16A voltage-dependent Cl^- current in proximal convoluted tubule cells is dynamically regulated by the renin-angiotensin system

kcne1 $^{-/-}$ and *tmem16a*$^{-/-}$ mice both exhibit an increased hematocrit value and dehydration due to enhanced water loss (Vallon et al., 2001; Faria et al., 2014), which suggests a functional role of the KCNE1-TMEM16A complex in water reabsorption and consequently in blood pressure regulation. In the renal proximal tubule, these processes are regulated by the renin-angiotensin system which activates AT1R leading to PKC pathway stimulation. This pathway increases Na^+ transport through activation of the apical Na^+/H^+ exchanger 3 (NHE3) (Harris and Young, 1977; Lara et al., 2008; Li et al., 2011). To keep the electroneutrality, Na^+ transport needs notably Cl^- as a counter ion. We hypothesized that the KCNE1-TMEM16A channels carry this Cl^- current

Application of angiotensin II (AngII), the natural ligand of Angiotensin II Receptor type 1 (AT1R), on wild type PCT cells led to a ~3-fold increase in chloride current with a reversal potential that was similar to the expected Cl^- reversal potential (**Figure 5A)**. AngII application on *kcne1*$^{-/-}$ PCT cells failed to produce any current increase (6.5 ± 0.6 pA/pF vs 6.6 ± 1.1 pA/pF, $P > 0.9$, **Figure 5B)**, demonstrating that this AngII-induced chloride current is dependent on KCNE1. Moreover, knock-down of TMEM16A by siRNA transfection (Sala-Rabanal et al., 2017) in wild type PCT cells prevented this Cl^- current increase (9.21 ± 1.07 pA/pF vs 10.03 ± 1.1 pA/pF, **Figure 5C)** and Ani9 application fully inhibited it (68.69 ± 8.77 vs 8.92 ± 1.25 pA/pF, **Figure 5D**). Together this demonstrates that the Cl^- current enhanced by AngII is dependent on KCNE1 and is carried by TMEM16A, showing an endogenous role for the KCNE1-TMEM16A channel in the renin-angiotensin system.

In the proximal tubule, AT1R has been shown to couple to protein kinase A (PKA) (Crajoinas et al., 2016) and protein kinase C (PKC) (Lara et al., 2008) pathways. As shown in

Figure S5A, application of the PKA agonist 8-(4-Chlorophenylthio) adenosine 3',5'-cyclic monophosphate (CPT-cAMP) on wild type PCT cells did not alter the Cl^- current (21.60 ± 3.03 pA/pF vs 19.69 ± 20.3 pA/pF, P > 0.5), whereas phorbol 12-myristate 13-acetate (PMA), a PKC agonist, led to a similar Cl^- current increase as observed for AT1R activation (27.13 ± 2.04 pA/pF vs 83.47 ± 14.81 pA/pF, **Figure S5B**). This indicates that AT1R activates the PKC pathway to enhance the KCNE1-TMEM16A current. Moreover, this regulation is KCNE1-dependent, since *kcne1*$^{-/-}$ PCT cells did not respond to PMA (5.59 ± 1.14 pA/pF vs 9.19 ± 1.97 pA/pF, P > 0.1, **Figure S5C**), as it was also seen for AngII.

To address how KCNE1 confers the ability of the TMEM16A Cl^- current to be activated by AngII through the PKC pathway, we reconstituted the system in HEK293T cells allowing to control protein expression. First, we validated the model: AngII did not modify the TMEM16A current when co-expressed with AT1R alone (**Figure S6A**) but induced a ~2.5-fold increase of the TMEM16A-KCNE1 chloride current on cells co-expressing KCNE1-TMEM16A and AT1R (**Figure S6B**). As observed in PCT cells, PMA, but not CPT-cAMP, induced a ~3-fold increase of the TMEM16A-KCNE1 chloride current (20.31 ± 3.31 vs 63.12 ± 10.39 pA/pF, **Figure S6C and S6D**), confirming an involvement of PKC. Substitution of the KCNE1-serine S102, a known PKC-targeted residue (Kanda et al., 2011; Xu et al., 2009), by an alanine abolished the regulation of the channel by AT1R and PKC (**Figure S7A and S7B**). Therefore, it is the phosphorylation of KCNE1 at residue S102 that promotes the TMEM16A-KCNE1 current following AT1R and PKC activation. Furthermore, replacement of S102 by an aspartate residue, mimicking a phosphorylated serine (Kanda et al., 2011; Xu et al., 2009), induced a ~3.5-fold increase of the current (20.31 ± 3.31 vs 74.88 ± 24.38 pA/pF, **Figure S7C**) similar to the current increase induced by either PKC or AT1R activation, confirming the pivotal role of KCNE-S102 phosphorylation in the TMEM16A-KCNE chloride current regulation. These data demonstrate that in addition to the modification of channel gating, KCNE1 brings a new regulation to TMEM16A by AT1R through PKC activation.

The N-terminal pre-transmembrane domain of KCNE1 is key for TMEM16A regulation

KCNE1 is a single transmembrane protein with an extracellular N-terminal domain and a C-terminal domain within the cytosol (Takumi et al., 1988). To determine the interacting site with TMEM16A, we produced a series of truncated KCNE1 forms (**Figure 6A**) and tested them for their ability to regulate TMEM16A. Truncation of the KCNE1 C-terminal domain (the last 80 residues of the C-terminus) did not abolish the KCNE1-mediated TMEM16A regulation

(25.04 ± 4.9 pA/pF, P > 0.15; **Figure 6B**). By contrast, deletion of the full N-terminal domain suppressed the ability of KCNE1 to regulate TMEM16A (6.56 ± 0.89 pA/pF; **Figure 6B**). No effect was observed for the partial N-terminal truncations, neither for ΔNt16 (25.43 ± 4.46 pA/pF) nor for ΔNt30 (25.23 ± 6.62 pA/pF; **Figure 6C**). This demonstrates that the domain essential for TMEM16A activation is included in the sequence of the 13 residues preceding the transmembrane domain from L30 to L42. This result is in line with the previous observation, that a partial deletion of KCNE1, including eight of the 13 amino acids of this sequence ($KCNE1\Delta_{11-38}$), abolished the KCNE1-induced chloride current in *Xenopus* oocytes (Attali et al., 1993). To check if this small domain is sufficient to recapitulate the properties of the entire KCNE1 on the TMEM16A current, we used a corresponding synthetic peptide (Nter13), bearing the L30-L42 sequence. In HEK293T cells only expressing TMEM16A, application of 100 µM Nter13 elicited an Ani9-sensitive current (15.48 ± 3.25 pA/pF; **Figures 6D**, **S8A and S8B**). Again, the reversal potential was similar to the current observed when the full KCNE1 is co-expressed, whereas no effect was observed by application of a scrambled peptide (**Figure 6D**).

KCNE1 polymorphisms within the TMEM16A-interacting sequence suppress the Cl^- current

Previous works have identified two common KCNE1 polymorphisms, S38G and R32H, within the 13-residue extracellular domain. While these polymorphisms may be related to cardiac arrhythmia, they do not or just weakly affect the cardiac I_{Ks} current generated by KCNE1-KCNQ1 (Crump and Abbott, 2014; Westenskow et al., 2004; Yao et al., 2018, **Figure 7A and 7B**). We therefore tested the potential of these two KCNE1 variants to regulate TMEM16A. The disease-related mutation T7I, which does not belong to the regulating 13-residue domain, was used as a control. Whereas mutation T7I did not alter the KCNE1-dependent regulation of TMEM16A (24.69 ± 1.57 pA/pF; **Figures 7C and 7D**), both R32H and S38G mutations abolished the ability of KCNE1 to modulate the TMEM16A current properties (5.69 ± 1.18 pA/pF and 6.96 ± 0.78 pA/pF for R32H and S38G; **Figures 7C and 7D**). This finding suggests a potential role of the KCNE1-TMEM16A complex in human diseases.

DISCUSSION

Most ion channels are assembled as complexes of a pore-forming α-subunit, associated with auxiliary (β) subunits. In this study, we demonstrate that KCNE1, classically considered as a β-subunit of the cardiac KCNQ1 pore-forming subunit belonging to the voltage-dependent K_v channel superfamily, also serves as an auxiliary subunit of the anoctamin superfamily channel TMEM16A, a Ca^{2+}-activated Cl^- channel (CaCC). By stably interacting with TMEM16A following a 2α:2β stoichiometry, KCNE1 induces a voltage-dependent current in the absence of intracellular elevation of calcium. Furthermore, we show that the presence of KCNE1 in the TMEM16A channel complex is essential for the dynamic regulation by the blood pressure-regulating renin-angiotensin system in proximal tubule cells. KCNE1 polymorphisms within the TMEM16A-interacting domain abolish its ability to regulate TMEM16A, suggesting a possible implication of this voltage-dependent chloride current in human diseases.

β-subunits of ion channels are important molecular players providing a source of electrical signaling diversity in cells. Although they cannot induce native currents *per se*, they associate with pore-forming subunits of ion channels and modulate their pharmacological and biophysical characteristics. Their physiological importance is reflected by the large number of diseases linked to their mutations, such as muscular pathologies, epilepsy and cardiac arrhythmias (Adelman, 1995; Cannon, 2007; Crump and Abbott, 2014; Vergult et al., 2015). KCNE1 is a famous example of a K_v β-subunit, which associates with KCNQ1 and hERG to control both I_{Ks} and I_{Kr} components of the cardiac action potential. More than sixty KCNE1 gene variants have been reported to be associated with human diseases, particularly with cardiac arrhythmias (Crump and Abbott, 2014). Cross-modulation by β-subunits of pore-forming α-subunits from the same superfamily of ion channels was shown for Na_v and K_v channels (Marionneau et al., 2012; Nguyen et al., 2012). $Na_v\beta_1$ coordinates the control of K_v and Na_v channels, which derivate from the same ancestor (Moran et al., 2015) and belong to the superfamily of voltage-gated ion channels. Our results demonstrate auxiliary subunit-cross-modulation of two different superfamilies, which are phylogenetically not related: the voltage-gated channels and the anoctamins.

This cross-regulation concerns not only the KCNE member 1 of the KCNE subunit family, but also the KCNE member 5. Despite the fact that we do not find a significant alignment of the KCNE1's 13 residues sequence in the KCNE5 sequence, both subunits interact with TMEM16A and both seem to have a similar activating effect on the Cl^- current. A similar

effect does not necessarily mean an identical mode of action and it is possible that they differ in their manner to regulate TMEM16A. This has been already described for K_v channel regulation by the different KCNE members. For instance, both KCNE4 and KCNE5 provoke the same inhibition of KCNQ1 channels, but while KCNE4 inhibits the binding of the channel activator calmodulin, KCNE5 shifts the voltage-dependence of KCNQ1 toward highly depolarized potentials (Angelo et al., 2002; Ciampa et al., 2011) rendering the channel non-functional at physiological potentials. Future studies will aim to fully characterize these regulations and interactions between KCNE and TMEM16 members. Our results demonstrate auxiliary subunit-cross-modulation of two different superfamilies, which are phylogenetically not related: the voltage-gated channels and the anoctamins.

We found that, by interacting with TMEM16A, KCNE1 modifies the gating of this anoctamin member, switching it from a calcium-dependent to a voltage-dependent channel. Our experiments with different Ca^{2+} chelators and with the Ca^{2+}-activated SK4 channel as a very sensitive reporter demonstrated that activation of this CaCC is independent from any rise of cytosolic Ca^{2+}, the natural activator of the channel in the absence of KCNE1 (Caputo et al., 2008; Schroeder et al., 2008; Yang et al., 2008). We also discarded a potential increase of cell surface expression of TMEM16A when KCNE1 is present. An absent current density increase at a saturating Ca^{2+} concentration in the presence of KCNE1 shows that this protein does not stabilize the channel at the cell surface, as it was previously described for CLCA1 (Sala-Rabanal et al., 2017), but rather modifies channel gating. Recently, the TMEM16A-TM6 segment was reported to play a crucial role in voltage and calcium sensing (Peters et al., 2018). The TM6 was shown to be flexible allowing it to adopt several stable conformations that would condition the channel activity mode. Its key function was demonstrated by showing that two mutations within the TM6 (I637A and Q645A) enable channel activation by membrane depolarization in the absence of calcium, as KCNE1 does (Peters et al., 2018). The absence of an additive effect of KCNE1 when co-expressed with the two TM6 mutants supports an overlapping mechanism. KCNE1 may modulate channel activity by modifying the TM6 conformation, placing the channel in a voltage-dependent mode and enabling the channel to be activated independently of Ca^{2+}. Clearly, the voltage-dependent chloride channel superfamily is not restricted to the ClC family, but extends to the anoctamin family when combined with KCNE1. This also shows that the difference between Ca^{2+} and voltage-dependent channels is not strict and that we should rather consider a continuum of biophysical properties.

Whereas the KCNQ1-KCNE1 stoichiometry remains a matter of debate (Morin and Kobertz, 2008; Murray et al., 2016; Nakajo et al., 2010; Plant et al., 2014), we found that the TMEM16A-KCNE1 complex is composed of 2α:2β subunits by using the SiMPull assay. We have shown that this complex is formed in HEK cells upon heterologous expression, but we also demonstrated its presence in native kidney cells, where it mediates a Cl^- conductance which is sensitive to TMEM16A inhibitors. This Cl^- conductance cannot be recorded in KCNE1 knock-out cells or in cells in which TMEM16A has been knocked-down, and it is rescued in these cells by KCNE1 re-expression upon transfection. The TMEM16A-KCNE1 channel may participate in the volume regulation of PCT cells, as the regulatory volume decrease (RVD) typically observed after a hypo-osmotic shock in cells issued from *kcne1* $^{-/-}$ mice is reduced (Barrière et al., 2003). This lack of RVD was attributed to the loss of a chloride conductance and not to the loss of the KCNQ1-KCNE1 K^+ current, as it was anticipated at that time. At the whole animal level, *kcne1*$^{-/-}$ and *tmem16a*$^{-/-}$ mice exhibit similar phenotypes such as an increased hematocrit value and dehydration due to enhanced water loss (Vallon et al., 2001; Faria et al., 2014). The renin-angiotensin system is involved in blood pressure regulation by notably increasing water and salt reabsorption through activation of AT1R, enhancing the transport of Na^+ and its counter ion Cl^-. In line with this, our results demonstrate that the KCNE1-TMEM16A chloride current in proximal tubule cells increases upon activation of the renin-angiotensin system. This indicates that the KCNE1-TMEM16A chloride current is, at least partially, the AngII-dependent Cl^- KCNE1-TMEM16A current, in which TMEM16A is the pore-forming α-subunit and KCNE1 the β-subunit. Therefore, TMEM16A-KCNE1 association is not only found upon recombinant overexpression, but can also be observed in native cells, notably in renal PCT cells, in which the complex responds to the renin-angiotensin system involved in physiological blood pressure regulation.

Our detailed study of the signaling pathway, linking the renin-angiotensin system activation to the Cl^- TMEM16-KCNE1 current, demonstrates that it is the phosphorylation of the KCNE1 β-subunit which confers the ability to TMEM16A α-subunit to be stimulated by AngII. In fact, phosphorylation of KCNE1-S102 is responsible for the totality of the effect observed upon AngII binding on AT1R. Therefore, KCNE1 mediates a new dynamic channel regulation by involving intracellular PKC dependent pathways. Interestingly, the PKC-targeted S102 residue was shown to lead to a reduced I_{Ks} current, carried by KCNQ1-KCNE1 complex, when phosphorylated (Kanda et al., 2011; Xu et al., 2009).

Our electrophysiological assays, using truncated forms of KCNE1 and synthetic peptides based on the β-subunit, allowed us to determine the crucial role of the N-terminus of KCNE1 in TMEM16A regulation. More specifically, we have observed that the segment closer to the transmembrane domain of KCNE1 is necessary and sufficient to recapitulate the action of the entire KCNE1 on the TMEM16A current. The synthetic peptide generated on the basis of this segment's sequence is the first designed TMEM16A agonist and may be useful for clinical applications. Notably, activation of an apical chloride channel such as TMEM16A triggers the secretion of water, which makes TMEM16A-targeted activators potential drug candidates for treatment of cystic fibrosis or dry eye syndromes.

The KCNE1 N-terminal 13-amino acid segment bears at least two residues which are subject to polymorphisms (R32H and S38G) related with cardiac arrhythmias (Crump and Abbott, 2014). Whereas several clinically relevant KCNE1 variants were found to modify its ability to regulate KCNQ1, providing a link between these mutations and polymorphisms with cardiac arrhythmias, the KCNE1 S38G poorly impairs KCNQ1 regulation by KCNE1 (Yao et al., 2018). We found that the KCNE1 S38G as well as the R32H mutants lost their ability to regulate TMEM16A, suggesting a potential role of this chloride current in cardiac arrhythmias. Along this line, a recent study performed in canine heart suggests a protective role for TMEM16A against risk of arrhythmias by reducing spatial and temporal heterogeneity of cardiac repolarization and early after-depolarization (Hegyi et al., 2017).

To sum up, we have found that KCNE1, a well-known auxiliary subunit of voltage-dependent K^+ channels, fulfills the four needed conditions to be considered as an auxiliary subunit of the anoctamin anion channel superfamily (Adelman, 1995; Arikkath and Campbell, 2003; Cannon, 2007; Gurnett and Campbell, 1996; Trimmer, 1998): first, KCNE1 does not show any ion channel activity by itself, second, KCNE1 and TMEM16A interact directly and stably with a fixed stoichiometry (2α:2β), third, KCNE1 modifies drastically the TMEM16A function enabling the channel to work in the absence of elevated cytosolic calcium, and fourth, KCNE1 regulates TMEM16A in native tissue. Therefore, KCNE1 is a *bona fide* auxiliary subunit of two distinct classes of ion channel superfamilies which are not phylogenetically related: the voltage-gated cation channel and the anoctamin superfamily. Finally, the TMEM16A-KCNE1 association should be considered when analyzing outcomes of clinically relevant KCNE1 mutations, as emphasized by the finding that two known cardiac arrhythmia-related KCNE1 variants, including S38G, lost their ability to regulate TMEM16A.

ACKNOWLEDGMENTS

We thank Pr Lily Yeh Jan for providing us the clone encoding TMEM16A-GFP (isoform a) (RefSeq NM_001242349.1) and Pr Criss Hartzell for sharing the clone encoding the TMEM16A $_{444}$EEEE$_{447}$/$_{444}$AAAA$_{447}$ mutant. We also thank Pr Josh Levitz, Pr Harald Janovjak and Dr Michel Vivaudou for fruitful discussion. This work was supported by a grant to G.S. by the Fondation pour la Recherche Medicale (Equipe labellisée FRM 2017, FRM DEQ20170336753) the Agence Nationale pour la Recherche (AT2R-TRAAK-Bioanalgesics ANR-17-CE18-0001 and ANR-17-ERC2-0023), the Laboratory of Excellence "Ion Channel Science and Therapeutics" (grant ANR-11-LABX-0015-01) and the French government, through the UCAJEDI Investments in the Future project managed by the National Research Agency (ANR) with the reference number ANR-15-IDEX-01. The work was also supported by grant to P.A.P. by the Fondation pour la Recherche Medicale (FRM 2019, FDT201904008083) and to SH (Ville de Nice) . This work was further supported by a grant from the Israel Science Foundation (ISF 1365/17) to B.A. The experiments requiring microscope imaging were performed at the PRISM facility, "PRISM – IBV- CNRS UMR 7277- INSERM U1091-UNS."

AUTHOR CONTRIBUTIONS

Conceptualization: P.A.P., S.H., J.B. and G.S., Methodology: P.A.P., S.H., J.B., B.A. and G.S. Investigation: P.A.P., B.W., S.H. and Y.C.; Resources: C.D., Writing – Original draft: P.A.P., S.H., J.B., B.A. and G.S.; Writing – Review and editing: P.A.P., S.H., J.B., B.A. and G.S.; Funding Acquisition: G.S.; Project Administration G.S.

DECLARATION OF INTERESTS

The authors declare no competing interest

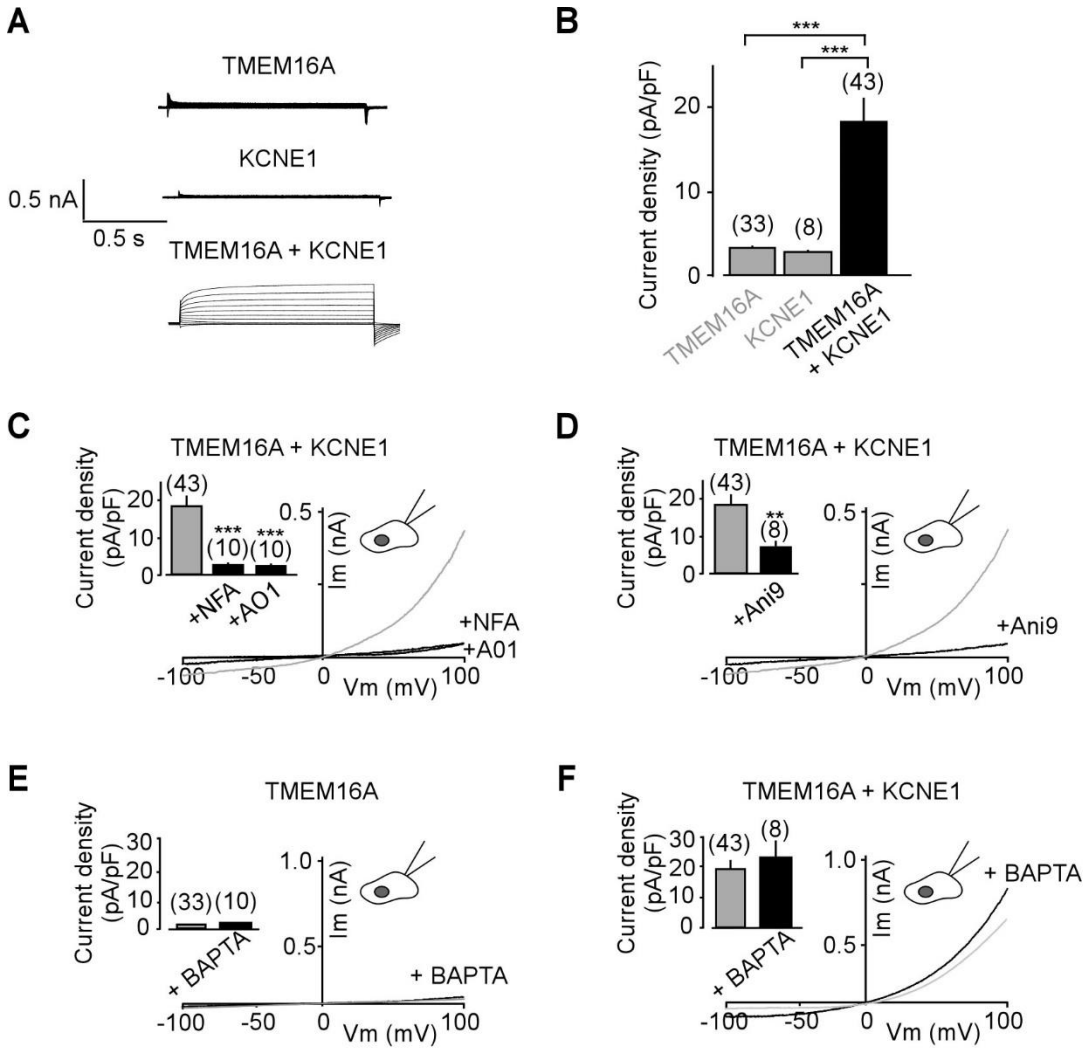

Figure 1. KCNE1 converts the CaCC TMEM16A into a voltage-dependent chloride channel. (A) Representative current traces showing the effect of expression of either KCNE1 or TMEM16A or both TMEM16A and KCNE1 in HEK293T cells. Traces were generated using pulses between -100 and +100 mV at 20 mV intervals from a holding potential of -80 mV. (B) Summary of current densities obtained at +100 mV. (C-D) Representative traces showing the effect of application of either niflumic acid (NFA, 100 µM, C), T16A(inh)A01 (10 µM, C) or Ani9 (300 nM, D). (E-F) Representative traces of TMEM16A alone (E) or co-expressed with KCNE1 (F) in the presence of 1 mM of BAPTA. Currents were elicited by voltage-ramps (from -100 to +100 mV, 1s duration), insets show a summary of current densities obtained at +100 mV. Mann-Whitney test (** $p < 0.01$, *** $p < 0.001$). Mean ± SEM.

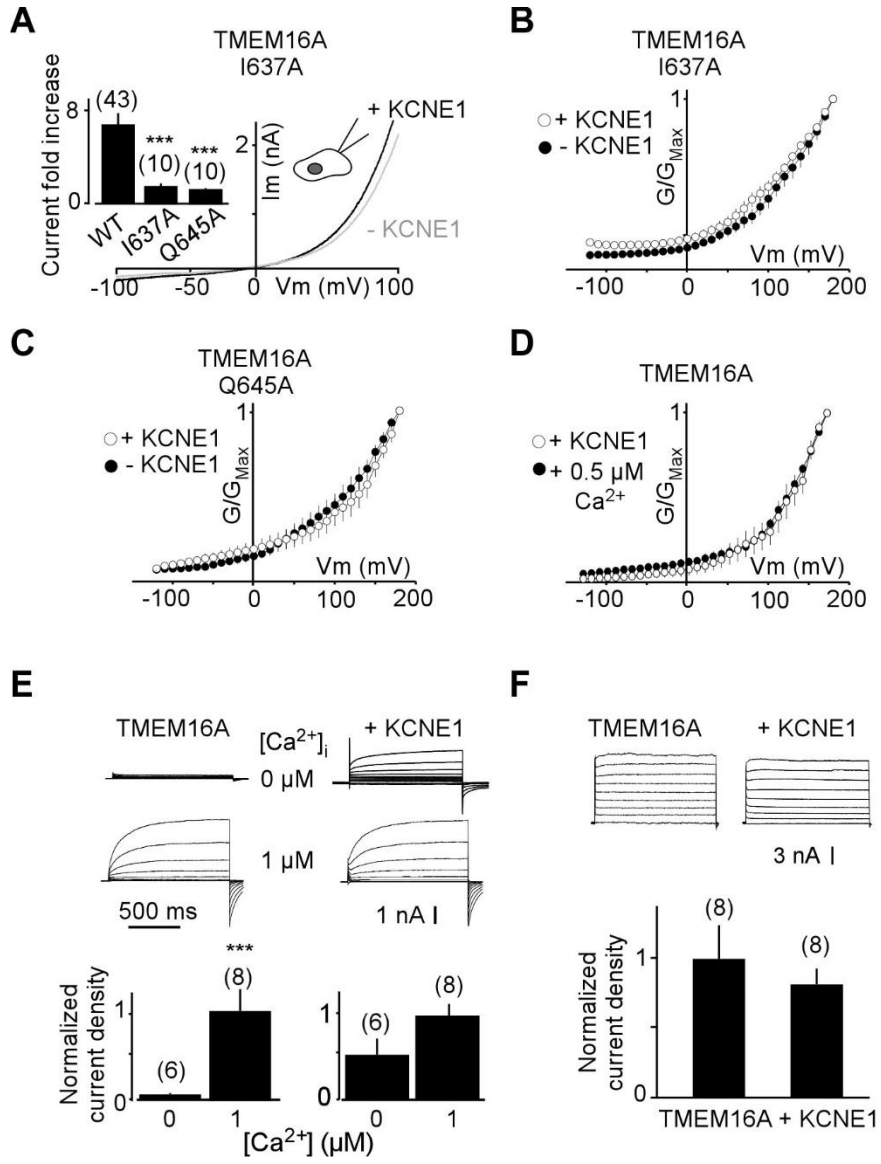

Figure 2. I637A and Q645A in the TM6 of TMEM16A are keys residues for channel regulation by KCNE1 and calcium. (A) Representative current traces showing the effect of expression of either TMEM16A I637A alone or TMEM16A I637A + KCNE1 in HEK293T cells. Currents were elicited by voltage-ramps (from -100 to +100 mV, 1s duration), insets show a summary of current density fold increase induced by KCNE1 co-expression at +100 mV in the wild type and TM6 mutant forms. (B-C) KCNE1 does not modify the voltage sensitivity of TMEM16A-TM6 I637A and Q645A mutants. G/G_{Max} vs Vm curves for I637A (B) and Q645A (C) mutants expressed alone or co-expressed with KCNE1 in whole-cell patch clamp. (D) TMEM16A activation at a moderate calcium concentration. G/G_{Max} vs Vm curves for TMEM16A alone in the presence of 0.5 µM Ca^{2+} and TMEM16A co-expressed with KCNE1. (E, F) Calcium sensitivity of TMEM16A-KCNE1 channel complex. (E) Whole cell current traces showing TMEM16A and TMEM16A + KCNE1 currents in the presence or absence of 1

µM $[Ca^{2+}]_i$. Bar graph represents relative current densities of TMEM16A and TMEM16A + KCNE1 at the two different calcium concentrations. (F) Sample traces from whole-cell patch-clamp recording of HEK293T cells expressing either TMEM16A alone or co-expressed with KCNE1, stepped from -80 to +80 mV in 20 mV steps from a holding potential of -80 mV at saturating $[Ca^{2+}]_i$. Bar graph represents normalized current densities of TMEM16A and TMEM16A + KCNE1 at a saturating calcium concentration showing a similar maximal current amplitude with or without KCNE1. Mann-Whitney test (*** $p < 0.001$). Mean ± SEM.

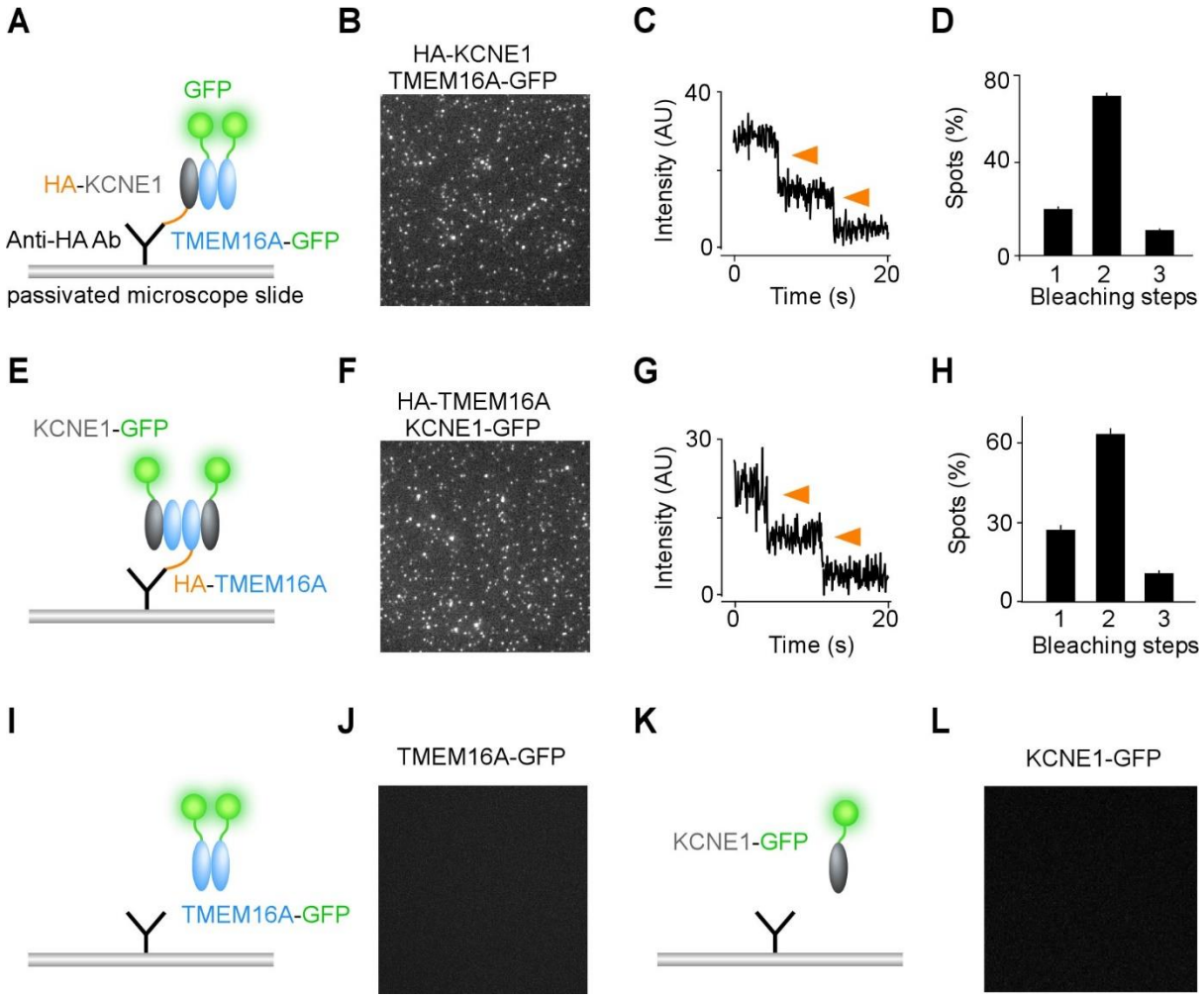

Figure 3. KCNE1 and TMEM16A interact in a 2α:2β complex. (A) Schematic of single molecule pulldown (SiMPull) assay of TMEM16A. Lysates of HEK293T cells co-expressing TMEM16A-GFP and HA-tagged KCNE1 were immobilized on a PEG-passivated coverslip conjugated to a biotinylated anti-HA antibody. (B) Representative TIRF image of single molecules showing the pulldown of TMEM16A-GFP by HA-KCNE1. (C) Representative trace showing two photobleaching steps (orange arrows) of TMEM16A-GFP (AU, for Arbitrary Units). (D) Summary of photobleaching step distribution for TMEM16A-GFP. (E-H), same as (A-D) for the SiMPull of KCNE1-GFP by HA-TMEM16A. (I-L) Specificity of the anti-HA antibody. (I-J) SiMPull assay with TMEM16A-GFP in the absence of HA-KCNE1. (K-L) SiMPull assay with KCNE1-GFP in the absence of HA-TMEM16A.

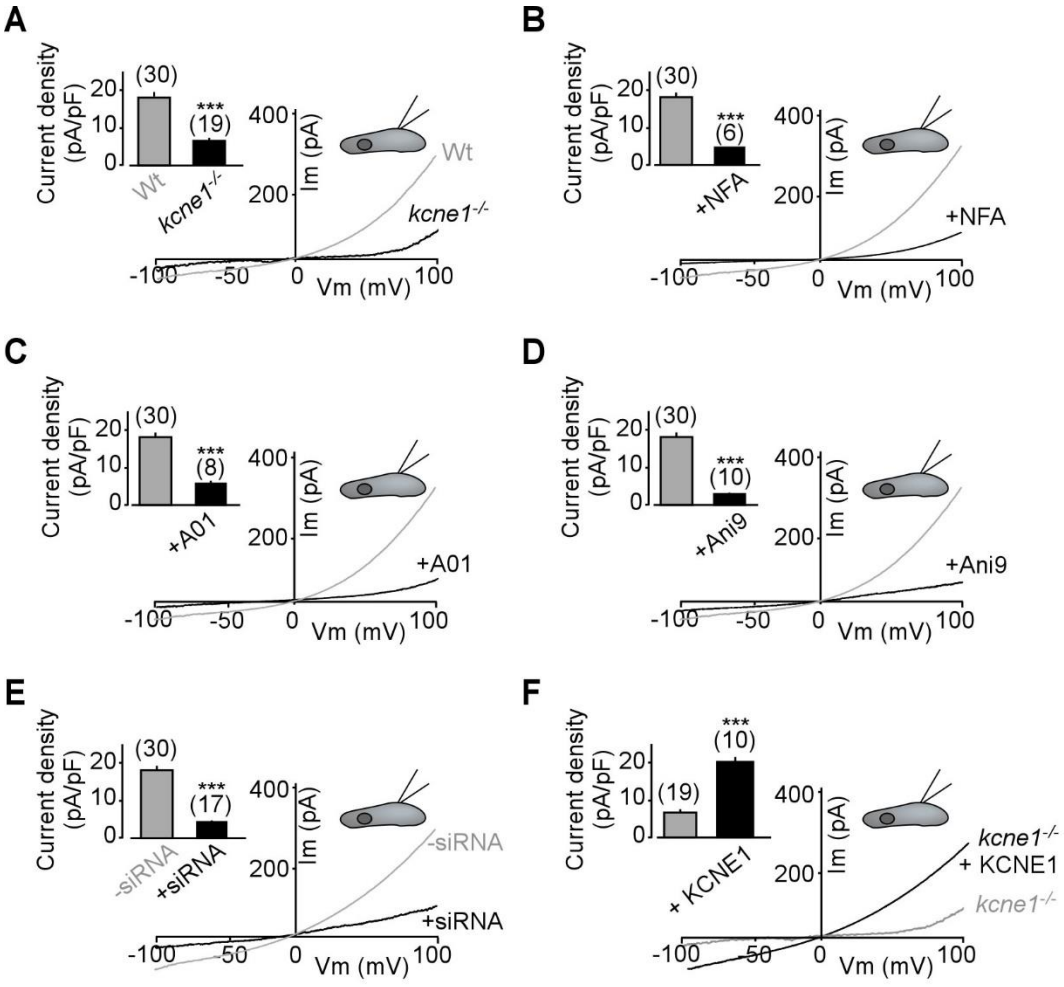

Figure 4. KCNE1-TMEM16A complex creates a voltage-dependent chloride current in proximal convoluted tubule (PCT) cells. (A) Representative traces obtained from wild type

and *kcne1*$^{-/-}$ PCT cells. (B-D) Representative traces from wild type cells after incubation with NFA (100 µM, B), A01 (10 µM, C), (5 µM Ani9, D). (E) Trace obtained after transfection with siRNA against TMEM16A. (F) Trace obtained from a *kcne1*$^{-/-}$ PCT cell after transfection with KCNE1 cDNA. Currents were generated by voltage-ramps (from -100 to +100 mV, 1s duration). Insets show current densities. Mann-Whitney test (*** $p < 0.001$). Mean ± SEM.

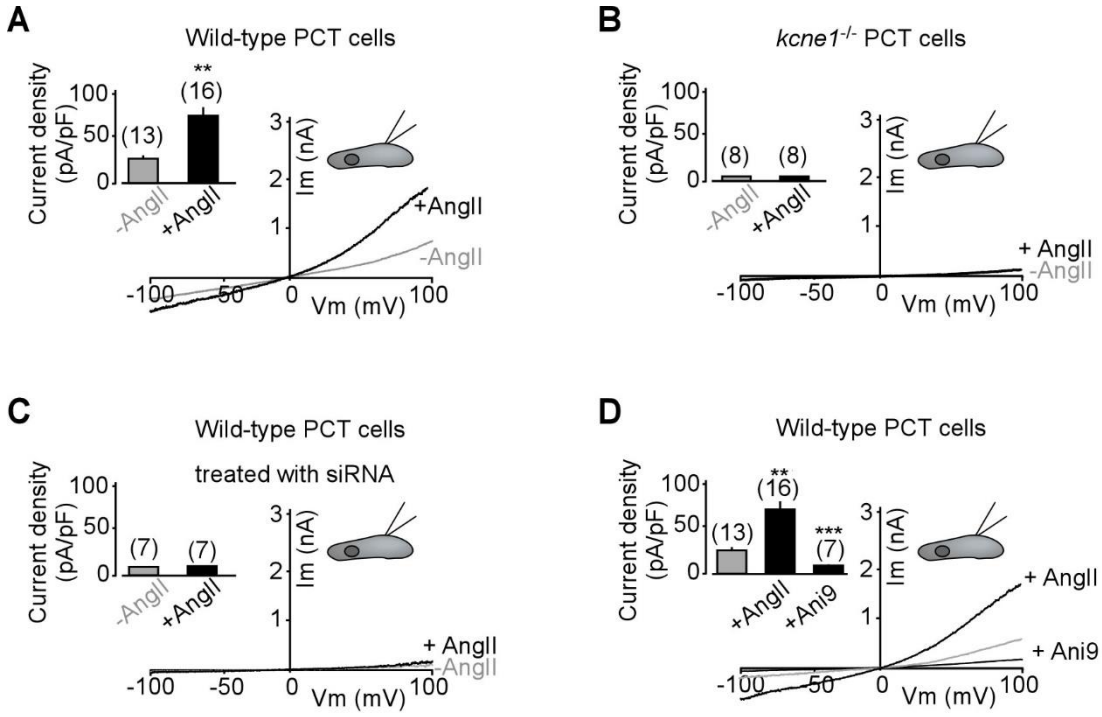

Figure 5. Activation of a KCNE1-dependent chloride current by the renin-angiotensin system in proximal tubule cells. (A-C) Representative current traces showing the effect of AngII application (100 nM) on wild type (A), *kcne1*$^{-/-}$ (B) and wild type PCT cells treated with a siRNA against TMEM16A (C). (D) Inhibition of wild type PCT cells stimulated with AngII by Ani9 (5 µM). Inset, current densities obtained at +100 mV. Representative traces of *kcne1*$^{-/-}$ PCT cells before and after treatment with AngII. Mann-Whitney test (** $p < 0.01$, *** $p < 0.001$). Mean ± SEM.

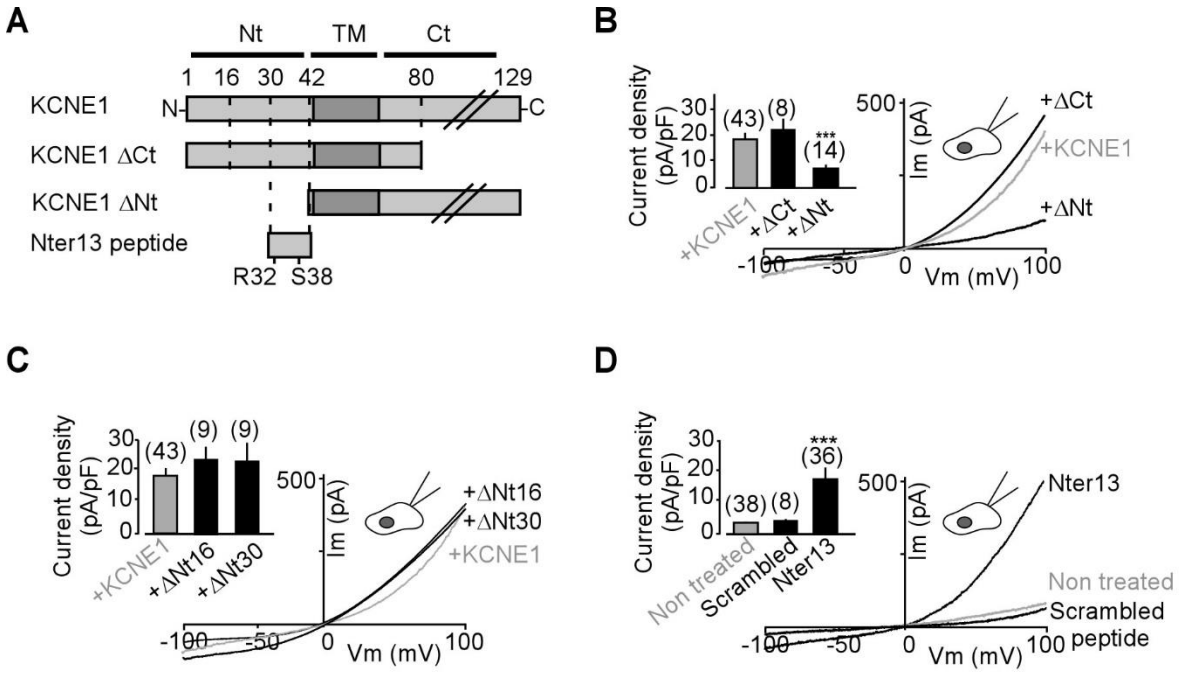

Figure 6. The pre-transmembrane domain (Nter13) of KCNE1 is sufficient for KCNE1-induced TMEM16A conversion. (A) Cartoon depicting KCNE1 truncated forms used to determine the domains implicated in TMEM16A interaction. (B-C) Representative traces obtained from HEK293T cells co-expressing TMEM16A and KCNE1ΔCt, KCNE1ΔNt (B), KCNE1ΔNt16, or KCNE1ΔNt30 (in which the first 16 and 30 residues were deleted, respectively, C). (D) Representative traces showing the effect of the Nter13 and a scrambled peptide on a HEK293T cell expressing TMEM16A alone. Currents were elicited by voltage-ramps (from -100 to +100 mV, 1s duration). Insets show the summary of current densities obtained for the different conditions at +100 mV. Mann-Whitney test (*** $p < 0.001$). Mean ± SEM.

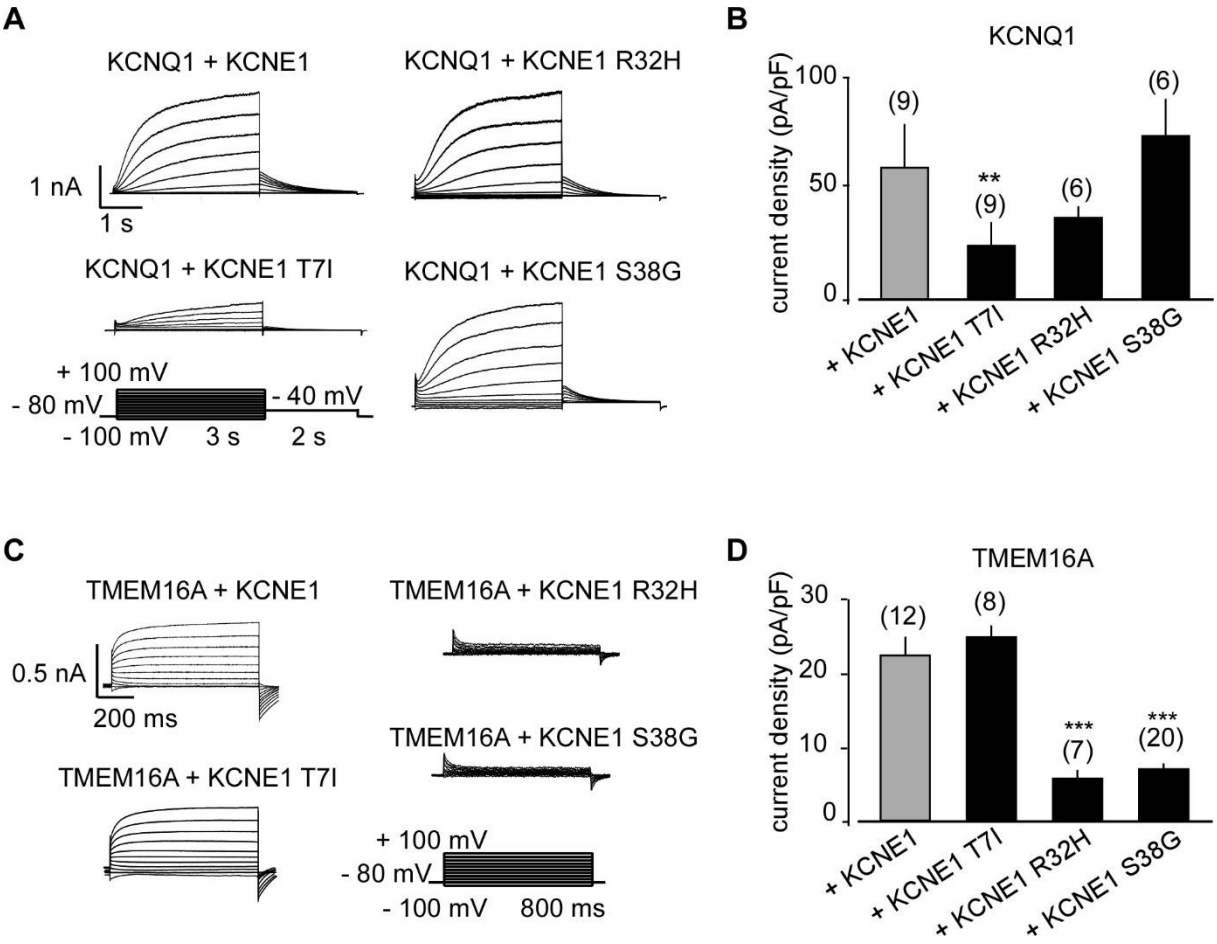

Figure 7. KCNE1 S38G and R32H do not impair the KCNQ1 regulation, but abolish TMEM16A regulation. (A) Current traces of whole-cell patch-clamp recordings from cells transfected with KCNQ1 alone and co-transfected with KCNE1 or KCNE1 R32H or KCNE1 S38G or KCNE1 T7I. (B) Summary of current densities obtained for the different conditions at +40 mV. (C-D) Same as (A-B), with cells co-expressing TMEM16A and the different KCNE1 forms. Current densities were calculated at +100 mV. Mann-Whitney test (** $p < 0.01$, *** $p < 0.001$). Mean ± SEM.

TABLE

Table 1. Relative permeabilities (P_x/P_{Cl}) of the TMEM16A-KCNE1 current to anions.

Salt	E_{rev}	*Relative permeability*	*n*
NaCl (140 mM)	-5.4 ± 1.4	1	11
NaI (140 mM)	-15 ± 2.8	1.5	6
$NaNO_3$ (140 mM)	-23.2 ± 1.4	2	5

STAR★Methods

KEY RESOURCES TABLE

REAGENT or RESOURCE	SOURCE	IDENTIFIER
Antibodies		
Biotinylated anti-HA clone 16B12	BioLegend	Cat# 901501
Collagen	Sigma-Aldrich	Cat# L2020
Lipofectamine 2000	Invitrogen	Cat#11668027
Moloney murine leukemia virus reverse transcriptase	Invitrogen	Cat# 28025013
NeutrAvidin	ThermoFisher	Cat# 31000
PEG	Laysan Bio	Item# MPEG-SVA-5000
Polybrene	Sigma-Aldrich	Cat# TR-1003
Poly-L-lysine	Sigma-Aldrich	Cat#P4707
Protease inhibitors	Roche Diagnostics	Cat#4693116001
Trypsin	Sigma-Aldrich	Cat# T1763
Experimental Models: Cell Lines		
HEK 293T	ATCC	Cat#CRL11268
Mouse PCT	Barrière et al., 2003	N/A
Oligonucleotides		
TMEM16A: forward:, TATCTCGAGACCATGAGGGTCCCCGAGAAGTA reverse: ATAGAATTCCTACAGCGCGTCCCCAT	This paper	N/A
TMEM16A I637A Internal forward: CTGAGCATCGCTATGCTGGGCAAG Internal reverse: GCCCAGCATAGCGATGCTCAGCTG	This paper	N/A
TMEM16A Q645A Internal forward: CAGCTAATCGCGAACAATCTCTTC Internal reverse: GAAGAGATTGTTCGCGATTAGCTGCTT	This paper	N/A

KCNE1: forward: TATGAATTCACCATGATCCTGTCTAACACCACA reverse: TAGTCGACTCATGGGGAAGGCTTCGTCTCAGGA	This paper	N/A
Recombinant DNA		
pcDNA3.1-X-GFP	This paper	N/A
pCMV-HA-X	Clontech	631604
pIRES2eGFP	Clontech	6029-1
Software and Algorithms		
Fiji/ImageJ	NIH	Version 1.8
pClamp	Molecular Devices	Version 10
SigmaPlot	Systat Software Inc.	Version 11
Other		
Axioplan 2 Imaging Microscope	Zeiss	https://www.micro-shop.zeiss.com/?s=16103145829fcb6&l=en&p=us&f=a&i=10027
Axopatch 200A amplifier	Molecular Devices	https://fr.moleculardevices.com/systems/axon-conventional-patch-clamp/axopatch-200a-amplifier#gref
Camera EMCCD iXon	Andor	https://andor.oxinst.com/products/ixon-emccd-cameras

CONTACT FOR REAGENT AND RESOURCE SHARING

Further information and requests for resources and reagents should be directed to and will be fulfilled by the Lead Contact, Guillaume Sandoz (sandoz@unice.fr).

EXPERIMENTAL MODEL AND SUBJECT DETAILS

Molecular biology, gene expression and cell culture

mTMEM16A (kindly provided by Dr Lily Yeh Jan) and hKCNE1 cDNA were subcloned in pIRES2eGFP, pcDNA3.1, pCDNA3.1-GFP and pCMV-HA vectors. Truncations and mutations were generated by PCR. For SiMPull experiments, HA-tags were fused to the N-terminus of sequences, whereas GFP-tags were fused to the C-terminal part. HEK293T and PCT cells were transiently co-transfected using Lipofectamine 2000 or the calcium phosphate method with a total amount of 1 and 3.5 µg of DNA, respectively, and seeded on 18 mm diameter coverslips. HEK cells were maintained in DMEM with 10 % FBS on poly-L-lysine-coated glass coverslips in 12 well plates. PCT cells from wild type and knock-out mice were prepared as described previously (Barrière et al., 2003) and maintained in F12 (Gibco) on collagen-coated glass coverslips.

Electrophysiology

HEK293T and PCT cell electrophysiology was performed 24 – 48 h after transfection. For whole-cell patch-clamp experiments, cells were recorded in a bath solution containing (in mM) 150 NaCl, 5 KCl, 2 $CaCl_2$ and 10 HEPES, pH 7.4. The glass pipettes (2-5 MΩ of resistance) were filled with (in mM) 5 NaCl, 135 CsCl, 2 $MgCl_2$, 5 EGTA, 10 HEPES, pH 7.3. Total calcium concentration was calculated with Maxchelator (maxchelator.standford.edu) for a temperature of 20 °C. HEK293T and PCT cells were recorded at room temperature in voltage-clamp mode using an Axopatch 200A (Molecular Devices) amplifier. Signals were filtered at 10 kHz and digitalized at 20 kHz. Whole-cell currents were elicited by voltage-ramps (from -100 to +100 mV, 1 s) and I-V stimulation pulses (from -100 to +100 mV in 20 mV increments, 1 s each pulse), holding the cells at -80 mV. Current densities were measured at +100 mV.

For inside-out recordings, the extracellular (pipette) solution contained (in mM) 140 NaCl, 10 HEPES and 0.1 EGTA. The intracellular (bath) solution had the same composition as the pipette solutions for recordings in absence of Ca^{2+}. A saturating Ca^{2+} solution (~20 µM Ca^{2+}) was prepared by adding 0.12 mM of $CaCl_2$ to the bath solution. Non-saturating solutions included (in mM) 1 EGTA and 0.59, 0.79, 0.89, 0.94 of $CaCl_2$ to obtain 0.1 µM, 0.25 µM, 0.5 µM and 1 µM free-Ca^{2+} solutions, respectively. The pH of inside-out solutions was adjusted to 7.4 with NaOH. Cell recordings, data acquisition and analysis of electrophysiology were performed using pClamp software (Molecular Devices).

For anion permeability experiments, cells were recorded using a pipette filled with CsCl 140 mM. The permeability ratio P_X/P_{Cl} was calculated from the reversal potential shift (ΔE_r)

given by the Goldman-Hodgkin-Katz equation (**Equation 1**), when replacing extracellular Cl^- with ion X^-,

Equation 1

$$\Delta E_r = E_{rX} - E_{rCl} = \frac{RT}{zF} \ln \frac{PX^-[X^-]_o}{PCl^-[Cl^-]_o}$$

in which, E_{rX} and E_{rCl} represent the reversal potentials of ions X^- and Cl^-, and $[X^-]_o$ and $[Cl^-]_o$ represent concentrations of ions X^- and Cl^- in the bath solution, respectively.

Single Molecule Pulldown assay

For SiMPull assays, we followed the protocol previously described by Jain et al., 2011. Briefly, HEK293T cells co-transfected with an HA-tagged bait protein and a GFP-fused prey protein (applying the widely used eGFP A206K mutant which greatly reduces homodimerization events, Zacharias et al., 2002) were lysed in a buffer containing (in mM): 150 NaCl, 10 Tris pH 7.5, 1 EDTA, protease inhibitor cocktail (Thermo Scientific) and 1.5% IGEPAL (Sigma). Lysates were collected and pulled-down on coverslips passivated with PEG (99%) and biotin-PEG (1%) and treated with neutravidin (1.4 mg/mL, Pierce) and biotinylated anti-HA antibody (15 nM, abcam, #ab26228). Several washes with T50 buffer (in mM: 50 NaCl, 10 Tris, 20 EDTA; 0.1 mg/mL BSA, pH 7.5) were performed to avoid unspecific protein binding. Finally, single molecule complexes were imaged using a 488 nm Argon laser in total internal reflection fluorescence microscopy with a 100x objective (Olympus). 13 x 13 μm^2 movies of 250 frames were acquired at frame rates of 10–30 Hz and analyzed using Fiji software (NIH). Multiple independent experiments were performed for each condition and only the spots which were fully bleached at the end of the illumination were considered. Representative data sets are presented to quantitatively compare the different conditions (minimum 15 movies per condition, at least 50 analyzed traces per movie).

REFERENCES

Adelman, J.P. (1995). Proteins that interact with the pore-forming subunits of voltage-gated ion channels. Curr Opin Neurobiol *5*, 286-295.

Angelo, K., Jespersen, T., Grunnet, M., Nielsen, M.S., Klaerke, D.A., and Olesen, S.P. (2002). KCNE5 induces time- and voltage-dependent modulation of the KCNQ1 current. Biophys J *83*, 1997-2006.

Arikkath, J., and Campbell, K.P. (2003). Auxiliary subunits: essential components of the voltage-gated calcium channel complex. Curr Opin Neurobiol *13*, 298-307.

Attali, B., Guillemare, E., Lesage, F., Honoré, E., Romey, G., Lazdunski, M., and Barhanin, J. (1993). The protein IsK is a dual activator of K+ and Cl- channels. Nature *365*, 850-852.

Barhanin, J., Lesage, F., Guillemare, E., Fink, M., Lazdunski, M., and Romey, G. (1996). K(V)LQT1 and lsK (minK) proteins associate to form the I(Ks) cardiac potassium current. Nature *384*, 78-80.

Barrière, H., Rubera, I., Belfodil, R., Tauc, M., Tonnerieux, N., Poujeol, C., Barhanin, J., and Poujeol, P. (2003). Swelling-activated chloride and potassium conductance in primary cultures of mouse proximal tubules. Implication of KCNE1 protein. J Membr Biol *193*, 153-170.

Bendahhou, S., Marionneau, C., Haurogne, K., Larroque, M.M., Derand, R., Szuts, V., Escande, D., Demolombe, S., and Barhanin, J. (2005). In vitro molecular interactions and distribution of KCNE family with KCNQ1 in the human heart. Cardiovasc Res *67*, 529-538.

Cannon, S.C. (2007). Physiologic principles underlying ion channelopathies. Neurotherapeutics *4*, 174-183.

Cao, Y.J., and Houamed, K.M. (1999). Activation of recombinant human SK4 channels by metal cations. FEBS Lett *446*, 137-141.

Caputo, A., Caci, E., Ferrera, L., Pedemonte, N., Barsanti, C., Sondo, E., Pfeffer, U., Ravazzolo, R., Zegarra-Moran, O., and Galietta, L.J. (2008). TMEM16A, a membrane protein associated with calcium-dependent chloride channel activity. Science *322*, 590-594.

Ciampa, E.J., Welch, R.C., Vanoye, C.G., and George, A.L. (2011). KCNE4 juxtamembrane region is required for interaction with calmodulin and for functional suppression of KCNQ1. J Biol Chem *286*, 4141-4149.

Crajoinas, R.O., Polidoro, J.Z., Carneiro de Morais, C.P., Castelo-Branco, R.C., and Girardi, A.C. (2016). Angiotensin II counteracts the effects of cAMP/PKA on NHE3 activity and phosphorylation in proximal tubule cells. Am J Physiol Cell Physiol *311*, C768-C776.

Crump, S.M., and Abbott, G.W. (2014). Arrhythmogenic KCNE gene variants: current knowledge and future challenges. Front Genet *5*, 3.

Dang, S., Feng, S., Tien, J., Peters, C.J., Bulkley, D., Lolicato, M., Zhao, J., Zuberbühler, K., Ye, W., Qi, L., *et al.* (2017). Cryo-EM structures of the TMEM16A calcium-activated chloride channel. Nature *552*, 426-429.

Davis, A.J., Shi, J., Pritchard, H.A., Chadha, P.S., Leblanc, N., Vasilikostas, G., Yao, Z., Verkman, A.S., Albert, A.P., and Greenwood, I.A. (2013). Potent vasorelaxant activity of the TMEM16A inhibitor T16A(inh) -A01. Br J Pharmacol *168*, 773-784.

Falzone, M.E., Malvezzi, M., Lee, B.C., and Accardi, A. (2018). Known structures and unknown mechanisms of TMEM16 scramblases and channels. J Gen Physiol *150*, 933-947.

Faria, D., Rock, J.R., Romao, A.M., Schweda, F., Bandulik, S., Witzgall, R., Schlatter, E., Heitzmann, D., Pavenstädt, H., Herrmann, E., *et al.* (2014). The calcium-activated chloride channel Anoctamin 1 contributes to the regulation of renal function. Kidney Int *85*, 1369-1381.

Goldstein, S.A., and Miller, C. (1991). Site-specific mutations in a minimal voltage-dependent K+ channel alter ion selectivity and open-channel block. Neuron *7*, 403-408.

Gurnett, C.A., and Campbell, K.P. (1996). Transmembrane auxiliary subunits of voltage-dependent ion channels. J Biol Chem *271*, 27975-27978.

Harris, P.J., and Young, J.A. (1977). Dose-dependent stimulation and inhibition of proximal tubular sodium reabsorption by angiotensin II in the rat kidney. Pflugers Arch *367*, 295-297.

Hartzell, C., Putzier, I., and Arreola, J. (2005). Calcium-activated chloride channels. Annu Rev Physiol *67*, 719-758.

Hegyi, B., Horváth, B., Váczi, K., Gönczi, M., Kistamás, K., Ruzsnavszky, F., Veress, R., Izu, L.T., Chen-Izu, Y., Bányász, T., *et al.* (2017). Ca. J Mol Cell Cardiol *109*, 27-37.

Jain, A., Liu, R., Ramani, B., Arauz, E., Ishitsuka, Y., Ragunathan, K., Park, J., Chen, J., Xiang, Y.K., and Ha, T. (2011). Probing cellular protein complexes using single-molecule pull-down. Nature *473*, 484-488.

Kanda, V.A., Purtell, K., and Abbott, G.W. (2011). Protein kinase C downregulates I(Ks) by stimulating KCNQ1-KCNE1 potassium channel endocytosis. Heart Rhythm *8*, 1641-1647.

Lara, L.S., Correa, J.S., Lavelle, A.B., Lopes, A.G., and Caruso-Neves, C. (2008). The angiotensin receptor type 1-Gq protein-phosphatidyl inositol phospholipase Cbeta-protein kinase C pathway is involved in activation of proximal tubule Na+-ATPase activity by angiotensin(1-7) in pig kidneys. Exp Physiol *93*, 639-647.

Lesage, F., Attali, B., Lakey, J., Honoré, E., Romey, G., Faurobert, E., Lazdunski, M., and Barhanin, J. (1993). Are Xenopus oocytes unique in displaying functional IsK channel heterologous expression? Receptors Channels *1*, 143-152.
Levitz, J., Royal, P., Comoglio, Y., Wdziekonski, B., Schaub, S., Clemens, D.M., Isacoff, E.Y., and Sandoz, G. (2016). Heterodimerization within the TREK channel subfamily produces a diverse family of highly regulated potassium channels. Proc Natl Acad Sci U S A *113*, 4194-4199.
Li, H., Weatherford, E.T., Davis, D.R., Keen, H.L., Grobe, J.L., Daugherty, A., Cassis, L.A., Allen, A.M., and Sigmund, C.D. (2011). Renal proximal tubule angiotensin AT1A receptors regulate blood pressure. Am J Physiol Regul Integr Comp Physiol *301*, R1067-1077.
Marionneau, C., Carrasquillo, Y., Norris, A.J., Townsend, R.R., Isom, L.L., Link, A.J., and Nerbonne, J.M. (2012). The sodium channel accessory subunit Navβ1 regulates neuronal excitability through modulation of repolarizing voltage-gated K^+ channels. J Neurosci *32*, 5716-5727.
Moran, Y., Barzilai, M.G., Liebeskind, B.J., and Zakon, H.H. (2015). Evolution of voltage-gated ion channels at the emergence of Metazoa. J Exp Biol *218*, 515-525.
Morin, T.J., and Kobertz, W.R. (2008). Counting membrane-embedded KCNE beta-subunits in functioning K+ channel complexes. Proc Natl Acad Sci U S A *105*, 1478-1482.
Murray, C.I., Westhoff, M., Eldstrom, J., Thompson, E., Emes, R., and Fedida, D. (2016). Unnatural amino acid photo-crosslinking of the IKs channel complex demonstrates a KCNE1:KCNQ1 stoichiometry of up to 4:4. Elife *5*.
Nakajo, K., Ulbrich, M.H., Kubo, Y., and Isacoff, E.Y. (2010). Stoichiometry of the KCNQ1 - KCNE1 ion channel complex. Proc Natl Acad Sci U S A *107*, 18862-18867.
Nguyen, H.M., Miyazaki, H., Hoshi, N., Smith, B.J., Nukina, N., Goldin, A.L., and Chandy, K.G. (2012). Modulation of voltage-gated K+ channels by the sodium channel β1 subunit. Proc Natl Acad Sci U S A *109*, 18577-18582.
Pedemonte, N., and Galietta, L.J. (2014). Structure and function of TMEM16 proteins (anoctamins). Physiol Rev *94*, 419-459.
Peters, C.J., Gilchrist, J.M., Tien, J., Bethel, N.P., Qi, L., Chen, T., Wang, L., Jan, Y.N., Grabe, M., and Jan, L.Y. (2018). The Sixth Transmembrane Segment Is a Major Gating Component of the TMEM16A Calcium-Activated Chloride Channel. Neuron *97*, 1063-1077.e1064.
Plant, L.D., Xiong, D., Dai, H., and Goldstein, S.A. (2014). Individual IKs channels at the surface of mammalian cells contain two KCNE1 accessory subunits. Proc Natl Acad Sci U S A *111*, E1438-1446.
Royal, P., Andres-Bilbe, A., Ávalos Prado, P., Verkest, C., Wdziekonski, B., Schaub, S., Baron, A., Lesage, F., Gasull, X., Levitz, J., *et al.* (2019). Migraine-Associated TRESK Mutations Increase Neuronal Excitability through Alternative Translation Initiation and Inhibition of TREK. Neuron *101*, 232-245.e236.
Sala-Rabanal, M., Yurtsever, Z., Berry, K.N., Nichols, C.G., and Brett, T.J. (2017). Modulation of TMEM16A channel activity by the von Willebrand factor type A (VWA) domain of the calcium-activated chloride channel regulator 1 (CLCA1). J Biol Chem *292*, 9164-9174.
Sanguinetti, M.C., Curran, M.E., Zou, A., Shen, J., Spector, P.S., Atkinson, D.L., and Keating, M.T. (1996). Coassembly of K(V)LQT1 and minK (IsK) proteins to form cardiac I(Ks) potassium channel. Nature *384*, 80-83.
Sanguinetti, M.C., Jiang, C., Curran, M.E., and Keating, M.T. (1995). A mechanistic link between an inherited and an acquired cardiac arrhythmia: HERG encodes the IKr potassium channel. Cell *81*, 299-307.
Schroeder, B.C., Cheng, T., Jan, Y.N., and Jan, L.Y. (2008). Expression cloning of TMEM16A as a calcium-activated chloride channel subunit. Cell *134*, 1019-1029.
Seo, Y., Lee, H.K., Park, J., Jeon, D.K., Jo, S., Jo, M., and Namkung, W. (2016). cAni9, A Novel Potent Small-Molecule ANO1 Inhibitor with Negligible Effect on ANO2. PLoS One *11*, e0155771.
Takumi, T., Ohkubo, H., and Nakanishi, S. (1988). Cloning of a membrane protein that induces a slow voltage-gated potassium current. Science *242*, 1042-1045.
Trimmer, J.S. (1998). Regulation of ion channel expression by cytoplasmic subunits. Curr Opin Neurobiol *8*, 370-374.
Ulbrich, M.H., and Isacoff, E.Y. (2007). Subunit counting in membrane-bound proteins. Nat Methods *4*, 319-321.
Vallon, V., Grahammer, F., Richter, K., Bleich, M., Lang, F., Barhanin, J., Völkl, H., and Warth, R. (2001). Role of KCNE1-dependent K+ fluxes in mouse proximal tubule. J Am Soc Nephrol *12*, 2003-2011.
Vergult, S., Dheedene, A., Meurs, A., Faes, F., Isidor, B., Janssens, S., Gautier, A., Le Caignec, C., and Menten, B. (2015). Genomic aberrations of the CACNA2D1 gene in three patients with epilepsy and intellectual disability. Eur J Hum Genet *23*, 628-632.
Wang, K.W., and Goldstein, S.A. (1995). Subunit composition of minK potassium channels. Neuron *14*, 1303-1309.
Westenskow, P., Splawski, I., Timothy, K.W., Keating, M.T., and Sanguinetti, M.C. (2004). Compound mutations: a common cause of severe long-QT syndrome. Circulation *109*, 1834-1841.

Wozniak, K.L., Phelps, W.A., Tembo, M., Lee, M.T., and Carlson, A.E. (2018). The TMEM16A channel mediates the fast polyspermy block in. J Gen Physiol *150*, 1249-1259.
Xiao, Q., Yu, K., Perez-Cornejo, P., Cui, Y., Arreola, J., and Hartzell, H.C. (2011). Voltage- and calcium-dependent gating of TMEM16A/Ano1 chloride channels are physically coupled by the first intracellular loop. Proc Natl Acad Sci U S A *108*, 8891-8896.
Xu, X., Kanda, V.A., Choi, E., Panaghie, G., Roepke, T.K., Gaeta, S.A., Christini, D.J., Lerner, D.J., and Abbott, G.W. (2009). MinK-dependent internalization of the IKs potassium channel. Cardiovasc Res *82*, 430-438.
Yang, Y.D., Cho, H., Koo, J.Y., Tak, M.H., Cho, Y., Shim, W.S., Park, S.P., Lee, J., Lee, B., Kim, B.M., *et al.* (2008). TMEM16A confers receptor-activated calcium-dependent chloride conductance. Nature *455*, 1210-1215.
Yao, H., Ji, C.C., Cheng, Y.J., Chen, X.M., Liu, L.J., Fan, J., and Wu, S.H. (2018). Mutation in KCNE1 associated to early repolarization syndrome by modulation of slowly activating delayed rectifier K. Exp Cell Res *363*, 315-320.
Zacharias, D.A., Violin, J.D., Newton, A.C., and Tsien, R.Y. (2002). Partitioning of lipid-modified monomeric GFPs into membrane microdomains of live cells. Science *296*, 913-916.